有机化学 DOI: 10.6023/cjoc202204026 研究论文
Chinese Journal of Organic Chemistry ARTICLE

一种基于氟硼二吡咯(BODIPY)衍生物的高选择性“Off-On”型 Cu^{2+}比色-荧光探针

赵小龙*,[a] 李宇晴[a] 郭亮武[a] 冉启元[a] 吴会慧[a]
张 祯[a] 苏瀛鹏[a] 周鹏鑫[a] 燕 娜[b]
([a]西北师范大学化学化工学院 教育部生态环境相关高分子重点实验室 兰州 730070)
([b]兰州大学药学院 兰州 730000)

摘要 开发了一种水溶性良好的荧光增强型氟硼二吡咯(BODIPY)探针 **BDP-2Z**. 在较宽的 pH 范围(pH=3.0～12.0)内探针对 Cu^{2+}表现出低检测限、快速响应、高灵敏度和选择性等优势. Cu^{2+}引起的颜色和荧光对比非常显著, 能实现Cu^{2+}的可视化检测. 通过柱层析法分离得到识别过程的水解产物, 并利用紫外和荧光光谱、质谱分析证实了识别机制. 此外, 在真实水样中的快速裸眼识别扩展了其在环境检测方面的应用.

关键词 水溶性; 可视化; BODIPY 衍生物; 荧光增强

A Highly Selective and High-Contrast Colorimetric “Off-On” Chemosensor for Cu^{2+} Based on Boron-Dipyrromethene (BODIPY) Derivatives

Zhao, Xiaolong*,[a] Li, Yuqing[a] Guo, Liangwu[a] Ran, Qiyuan[a] Wu, Huihui[a]
Zhang, Zhen[a] Su, Yingpeng[a] Zhou, Pengxin[a] Yan, Na[b]
([a] *Key Laboratory of Eco-Environment-Related Polymer Materials*, *Ministry of Education*, *College of Chemistry and Chemical Engineering*, *Northwest Normal University*, *Lanzhou 730070*)
([b] *School of Pharmacy*, *Lanzhou University*, *Lanzhou 730000*)

Abstract Based on the platform of boron-dipyrromethene (BODIPY) derivatives, a fluorescence turn-on probe **BDP-2Z** was rationally designed and synthesized with good water-solubility. With high sensitivity and selectivity for Cu^{2+} over other competitive ions, the reaction-based probe showed low detection limit and fast response in a wide pH range (pH=3.0～12.0). The contrast of color and fluorescence caused by Cu^{2+} was remarkable so much so that it was easily to distinguish Cu^{2+} from other ions with naked-eye detection. Along with adding of Cu^{2+}, a blue shift of maximum absorption was observed from 548 nm to 496 nm, the corresponding solution color changed obviously from purple to light orange, and the fluorescence is enhanced by nearly 5-fold. Furthermore, the recognition mechanism was confirmed by UV-Vis, fluorescence spectra, and mass spectral analysis. The identified product of recognition process was even obtained by original silica gel column chromatography separation method. Also, the rapidly naked-eye application in real water samples provides an alternative to extension environmental detection.

Keywords water-soluble; naked-eye; BODIPY derivatives; fluorescence turn-on

1 Introduction

Copper is the third most abundant metal ion in the human body behind iron ions and zinc ions[1-2]. It is ubiquitous in nature and plays an critical role as an essential trace element in the body.[3] The deficiency of copper is closely related to diseases such as indirect anemia, malnutrition, osteoporosis, Parkinson’s disease and Alzheimer’s disease, which can

* Corresponding author. E-mail: zhaoxl82@nwnu.edu.cn
Received April 11, 2022; revised July 6, 2022; published online July 20, 2022.
Project supported by the Gansu Provincial Industrial Support Program for Colleges (No. 2021CYZC-17), the Natural Science Foundation of Gansu Province (No. 21JR1RA227), and the National Natural Science Foundation of China (No. 21462039).
甘肃省高等学校产业支撑计划(No. 2021CYZC-17)、甘肃省自然科学基金(No. 21JR1RA227)、国家自然科学基金(No. 21462039)资助项目.

cause nervous system disorders or metabolic disorders.[4-6] With the development of urban industrialization, the environmental pollution caused by metal ions is increasingly serious, and copper ion is one of the main contaminating ions, which may cause soil and water pollution. In addition, based on the essential of copper ions in physiology and pathology, it is particularly meaningful to explore materials for convenient and rapid monitoring of Cu^{2+} in the natural environment and *in vivo*.

Compared with traditional methods such as atomic absorption spectroscopy and capillary electrophoresis,[7] fluorescent probes have the advantages of simple operation, fast response and high sensitivity.[8-9] In recent years, numerous fluorescent probes for identifying Cu^{2+} have been reported.[10-13] Due to the paramagnetic properties of bivalent copper, most of the probes are prone to fluorescence quenching and the background interference is commonly strong[14-15], while the fluorescence enhancement strategy is optimal. In order to improve probe performance, "turn on" type of fluorescent probes are designed for reducing the impact of the weakness.[16-17] For the large conjugated system, certain molecules such as azobenzene, anthraquinone,[18-19] rhodamine[20-21] and naphthalimide,[22] *etc*. were selected as colorimetric probe for the quickly and easily naked eye recognition.

Boron-dipyrromethene (BODIPY) fluorescent compounds have been widely used due to their high quantum yields and insusceptibility to environmental values.[23-24] These molecules exhibit unique properties, such as strong UV absorption, narrow fluorescence emission, high molar extinction coefficients and so on.[25-26] In addition, it is not sensitive to the value of solvent polarity and environment, and is quite stable to physiological environment.[27-28] In recent years, there are few reports in the literature about the use of BODIPY-based colorimetric and fluorescent probes for the detection of Cu^{2+}. Therefore, it is still very attractive to develop novel ratiometric fluorescent probes that can detect Cu^{2+} rapidly with high sensitivity.

Based on the above considerations, a colorimetric and fluorescent turn on fluorescent probe for Cu^{2+} was designed and synthesized based on the BODIPY skeleton (as shown in Scheme 1). The probe **BDP-2Z** was constituted with BODIPY fluorophores and hydrazones receptors which could easily be hydrolyzed into carbonyl compounds in the presence of Cu^{2+} ions. In addition, two triethylene glycol substituent groups were used to improve the solubility in water. Due to the intramolecular charge transfer (ICT) effect caused by C=N isomerism, fluorescence of **BDP-2Z** was quenched, while it was obviously enhanced when group of HN—N=C was hydrolyzed in the presence of Cu^{2+}. The hydrolyzate **BDP-2** in which ICT effect decreased and vanished, exhibited strong fluorescence, leading to dramatic "off-on" fluorescence enhancement. In addition, the application of **BDP-2Z** was investigated for analysing Cu^{2+} in actual water samples. The standard addition recovery test was carried out and the results showed good accuracy and precision (RSD (relative standard deviation)＜3%), and good recovery rate, which proves practicability and validity of the probe.

2 Results and discussion

The synthetic route of probe **BDP-2Z** was shown in Scheme 1. The compound **2TEG-CHO** was synthesized according to previously published methods.[29-30] **BDP-2** was obtained by a one-pot reaction of **2TEG-CHO** and 2,4-dimethylpyrrole in the presence of *p*-TsOH as catalyst, followed by oxidative dehydrogenation with 2,3-dichloro-5,6-dicyano-1,4-benzoquinone (DDQ) and complexation reaction with BF_3•OEt_2. Probe **BDP-2Z** was prepared with 2,4-dinitrophenylhydrazine and BDP-2 under mild conditions. The chemical structures of these compounds were confirmed with ^{1}H NMR, ^{13}C NMR, and high resolution mass spectroscopy (HRMS). Corresponding analytical characterization data were provided in the supporting information.

2.1 Spectral characteristics

The UV-Vis and fluorescence spectral of probe **BDP-2Z** was investigated compared to that of probe BDP-2, which was the expected hydrolysis product of **BDP-2Z**. As a strong electron-withdrawing group, the structure of 2,4-dinitrophenylhydrazine had expanded the conjugated degree of BODIPY. Comparing with UV-Vis and fluorescence spectra of **BDP-2**, those of **BDP-2Z** were red-shifted by 52 nm and 94 nm, respectively. **BDP-2** exhibited a strong absorption peak at 496 nm and an emission peak at 511 nm in *N*,*N*-dimethylformamide (DMF)/H_2O solution (5 μmol/L, pH=7.4, V∶V=9∶1), while **BDP-2Z** showed a strong absorption peak at 548 nm and relatively weak fluorescence at 550 nm. The fluorescence quenching was mainly owing to the isomerization of group Ar—C=N, which would aggravate the nonradiative transition of the excited state of the molecule, besides, ICT also leads to fluorescence quenching. In this situation, the "off" state of **BDP-2Z** with the reducible active site provided the possibility of fluorescence enhancement.

2.2 Spectroscopy selectivity study of probe towards metal ions

In the DMF-H_2O system (pH=7.4, V∶V=9∶1), the sensing ability and the selectivity of the probe **BDP-2Z** for Cu^{2+} and the selectivity of the probe were investigated by UV-Vis spectroscopy and fluorescence spectroscopy. All the 19 kinds of metals, except Cu^{2+}, did not cause any other significant change after adding 10 equiv. of 19 metal cations (Li^+, Ag^+, Al^{3+}, Ba^{2+}, Ca^{2+}, Cd^{2+}, Co^{2+}, Cu^{2+}, Cu^+, Fe^{3+}, Fe^{2+}, Hg^{2+}, K^+, Mg^{2+}, Na^+, Ni^{2+}, Cr^{3+}, Mn^{2+} and Zn^{2+}) to the probe. The maximum absorption of the blank sample and other competing ions was still observed at 548 nm as the original performance, and no color changes appeared. However, the absorption band was reduced and blue-shifted from 548 nm to 496 nm when Cu^{2+} was added immediately (Figure 1a). As shown in Figure 1b, the fluorescence of the mixture of probe **BDP-2Z** and various competing ions (10

equiv.) was weak under the excitation of 478 nm and there was no significant emission change in fluorescence. Once the Cu^{2+} was added in, the probe solution turned green immediately, showing a clear fluorescence enhancement nearly 5-fold at 510 nm (Figure 1c). At the same time, an obvious color change from purple to light orange could be observed under visible light, indicating that **BDP-2Z** could be used as a naked-eye indicator of Cu^{2+}(Figure 2).

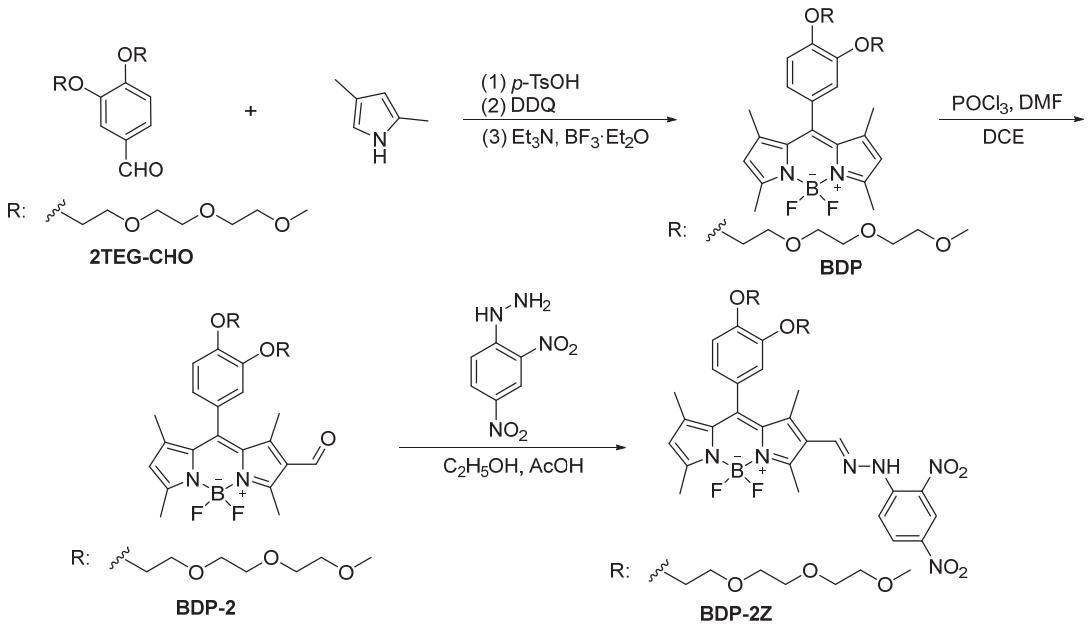

Scheme 1 Synthetic route of **BDP-2Z**

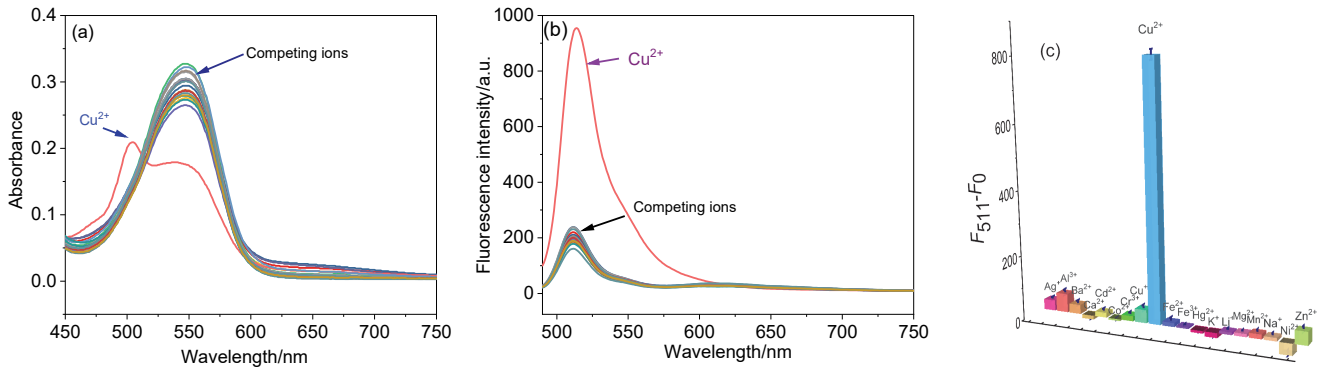

Figure 1 (a) UV-vis spectra of **BDP-2Z** (5 μmol/L) with addition of 10.0 equiv. of Cu^{2+} and the competing agents (Ag^{+}, Al^{3+}, Ba^{2+}, Ca^{2+}, Cd^{2+}, Co^{2+}, Cr^{3+}, Cu^{+}, Fe^{2+}, Fe^{3+}, Hg^{2+}, K^{+}, Li^{+}, Mg^{2+}, Mn^{2+}, Na^{+}, Ni^{2+}, Zn^{2+}) in DMF/H_2O (pH=7.4, V∶V=9∶1) solutions (λ_{ex}=478 nm); (b) fluorescence emission spectra of probe **BDP-2Z** (5 μmol/L) with 50 μmol/L of Cu^{2+} or 50 μmol/L of other ions; (c) emission intensity ratio (F_{511}/F_0) of **BDP-2Z** (5 μmol/L) in DMF/H_2O (pH=7.4, V∶V=9∶1) solutions in the presence of various species (50 μmol/L)

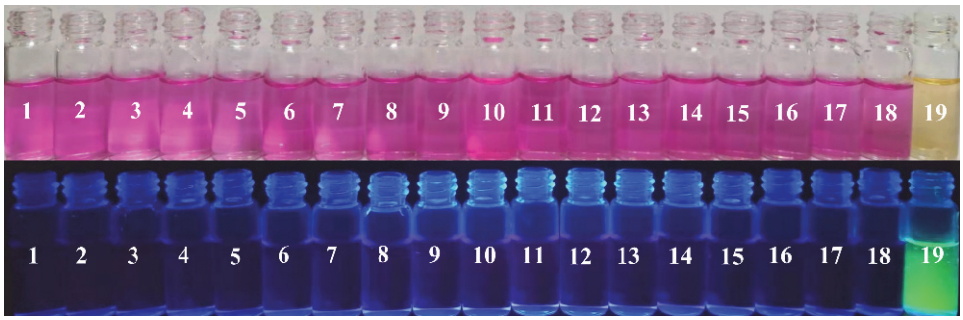

Figure 2 Colorimetric changes (up) and fluorescence photographs (down) of **BDP-2Z** (5 μmol/L) with 10 equiv. of different metal ions in DMF/H_2O (V∶V=9∶1) (including 1: Ag^{+}, 2: Al^{3+}, 3: Ba^{2+}, 4: Ca^{2+}, 5: Cd^{2+}, 6: Co^{2+}, 7: Cr^{3+}, 8: Cu^{+}, 9: Fe^{2+}, 10: Fe^{3+}, 11: Hg^{2+}, 12: K^{+}, 13: Li^{+}, 14: Mg^{2+}, 15: Mn^{2+}, 16: Na^{+}, 17: Ni^{2+}, 18: Zn^{2+}, 19: Cu^{2+})

To investigate the sensing capability to prevent interference in complex environments, simulated competition experiment was carried out by adding Cu^{2+} into to the mixture of **BDP-2Z** and competition ions (Figure 3). Originally the free probe showed quite weak fluorescence at 514 nm and there was no fluorescence transformation and colorimetric distinctions post adding of competitive ions. As expected, obvious enhancement of fluorescence was observed when the Cu^{2+} was added in, and the color turned light orange immediately compared to the initial purple. This results clearly demonstrated that the selectivity of **BDP-2Z** for Cu^{2+} was not significantly disturbed by common coexisting ions and the **BDP-2Z** showed more resilient to environmental disturbance. Notably, **BDP-2Z** could be naked-eyed recognition which had been a major obstacle in the development of ion detection.

2.3 UV-vis and fluorescence titration

The changes of the UV-Vis and fluorescence spectra were investigated by adding Cu^{2+} solutions gradually into increasing concentrations to the **BDP-2Z** solution. As shown in Figure 4a, the absorbance around 548 nm decreased, while a new peak at 496 nm belonging to BDP-2 appeared and increased when Cu^{2+} was added stepwise. This titration process proved a fact that the compound **BDP-2Z** was hydrolyzed to **BDP-2** in the presence of Cu^{2+}. In addition, the ratio of absorbance at 548 and 496 nm was plotted against Cu^{2+} concentration non-linearly (Figure 4b). To demonstrate the colorimetric response of **BDP-2Z** to Cu^{2+}, different concentrations of Cu^{2+} were added dropwise to the probe solution. As shown in Figure 4c, the color of the solution gradually became lighter in the range of 0, 5, 10, and 15 μmol/L. It was worth mentioning that the resolvable concentration of Cu^{2+} was as low as 5 μmol/L, indicating the probe combined ability of high-sensitivity detection of Cu^{2+}. This clearly distinguishable fluorescence response enables **BDP-2Z** to visually determine Cu^{2+} content.

As shown in Figure 5a, upon the increase of Cu^{2+} concentrations, the fluorescence intensity increased significantly at 511 nm and reached saturation when 10 equiv. of

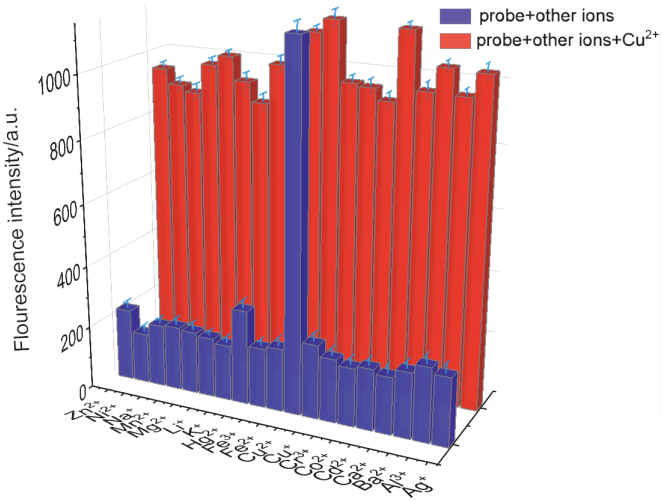

Figure 3 The blue bars represent the fluorescent intensity of sensor **BDP-2Z** and various metal ions (20 equiv.) in DMF/H_2O (V∶V=9∶1) solution; the red bars represent the fluorescent intensity of sensor **BDP-2Z** and Cu^{2+} (10 equiv.) in DMF/H_2O (V∶V=9∶1) solution

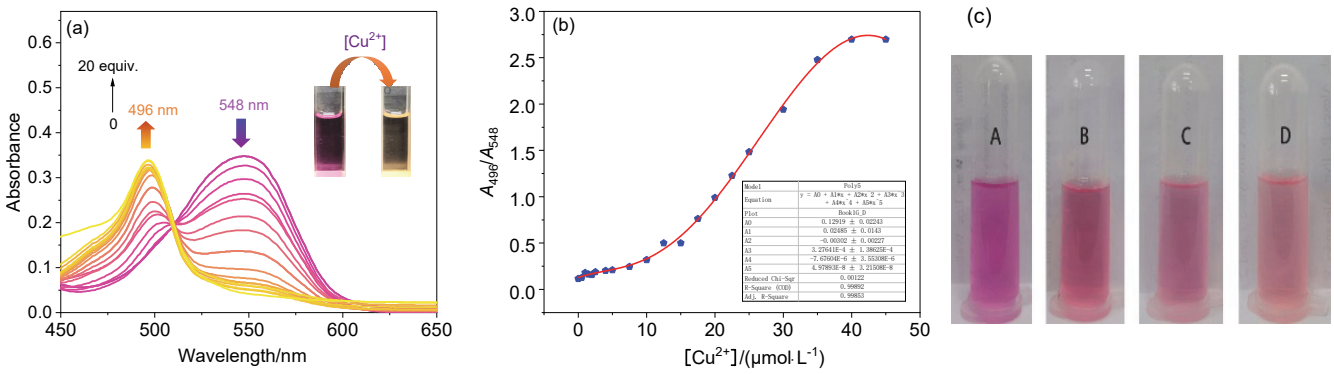

Figure 4 (a) UV-vis spectra of **BDP-2Z** in the presence of increasing concentration of Cu^{2+}over the range from 0 to 50 μmol/L (λ_{ex}=478 nm. Inset: images of **BDP-2Z** (pink, left) and in the absence Cu^{2+} under day light (orange, right)); (b) the relationship of A_{496}/A_{548} versus the concentration of Cu^{2+} over the range from 0 to 50 μmol/L (λ_{ex}=478 nm); (c) Color changes of **BDP-2Z** (5 μmol/L) in DMF/H_2O (V∶V=9∶1) upon addition of different concentration Cu^{2+}: 0 (A), 5 (B), 10 (C) and 15 (D) μmol/L

Cu^{2+} was added. Meanwhile, a clear emission color change (from dark red to green) could be easily observed. Furthermore, the relative relationship between normalized fluorescence intensity and Cu^{2+} concentration ($F-F_0$) showed a good linear relationship in the range of 0～5 μmol/L according to the fluorescence titration data (Figure 5b). The linear equation is $y=0.28369\times10^{-6}x+0.9459$ ($R^2=0.99595$), and the detection limit was determined to be 9.8×10^{-7} mol/L according to the definition of 3 times the blank signal deviation ($S/N=3$).

2.4 Effects of pH and time response

A short response time and pH suitability were another two important properties for a pragmatic fluorescent probe beside high sensitivity and selectivity. Therefore, time-dependent analysis of **BDP-2Z** was performed by fluorescence spectroscopy in the absence and presence of Cu^{2+} (10 equiv.). In order to dynamically monitor Cu^{2+} in environmental samples in real time, the time-dependent fluorescence intensity at 511 nm was recorded after the addition of Cu^{2+} (0, 2.5, 15, 50 μmol/L). The results showed that the fluorescence intensity increased to a constant value sharply and remained within 5 min after adding the Cu^{2+} (0, 2.5, 15, 50 μmol/L) to **BDP-2Z** (5 μmol/L), revealing a short response time to Cu^{2+} (Figure 6a).

The pH dependence of Cu^{2+} was also examined. As shown in Figure 6b, probe **BDP-2Z** exhibited stable weak fluorescence in a wide pH range (pH=3.0～12.0), while the fluorescence response of probe to Cu^{2+} was efficient and pH-dependent due to the protonation effect of C=N, in especial in the pH range of 6.0～9.0. This property allowed **BDP-2Z** to be an appropriate probe for rapid detecting environmental water samples during the biological pH range without being affected.

2.5. Sensor mechanism

To study the properties of **BDP-2Z** in depth, the sensing mechanism was hypothesized as follows: For the specific affinity to N atoms, Cu^{2+} could easily coordinate with the hydrazone to inhibit its isomerization and then promoted the cleavage of imine bonds to produce **BDP-2** by the hydrolysate of **BDP-2Z**. The fluorescence of **BDP-2Z** was

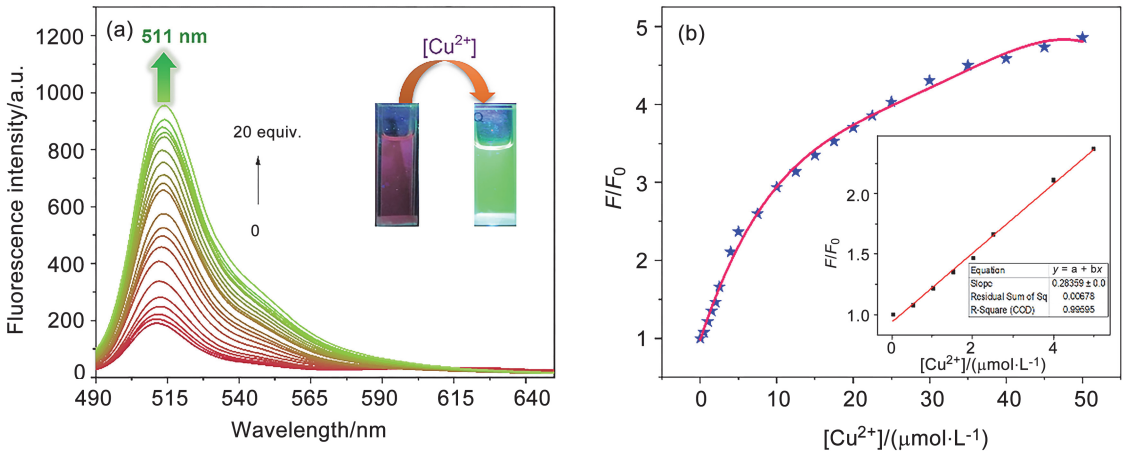

Figure 5 (a) Fluorescence response of **BDP-2Z** in the presence of increasing concentration of Cu^{2+}over the range from 0 to 50 μmol/L (λ_{ex}=478 nm); (b) the relationship of F_{511}/F_0 versus the concentration of Cu^{2+} over the range from 0 to 50 μmol/L (λ_{ex}=478 nm)

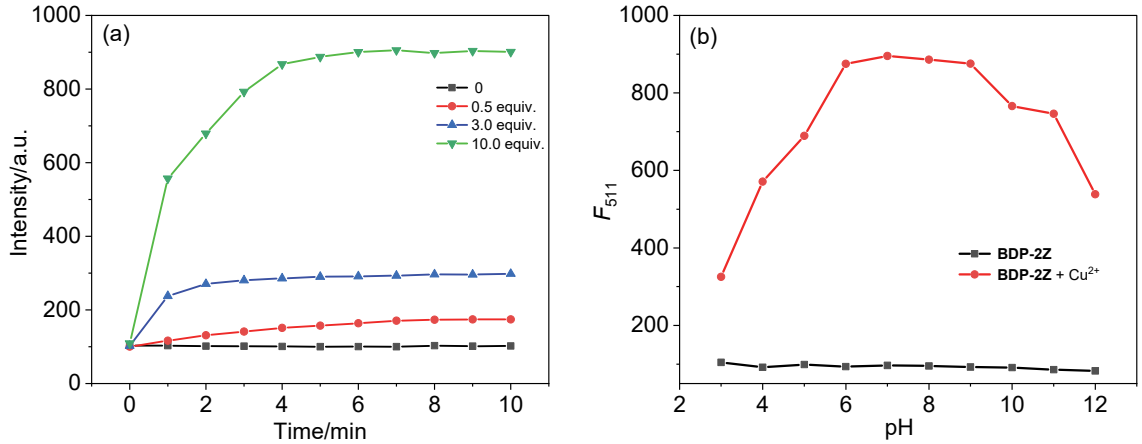

Figure 6 (a) Fluorescence response of probe **BDP-2Z** (5 μmol/L) in presence of different concentrations of Cu^{2+} ion; (b) the fluorescence intensity changed at 511 nm of probe **BDP-2Z** (5 μmol/L) in the absence and presence of 10.0 equiv. Cu^{2+} in DMF/H_2O (V/V=9/1). The pH was modulated by adding 0.1 mol/L HCl or 0.1 mol/L NaOH

initially quenched and then turned on due to the "on-off" conversion of ICT effect (Scheme 2). To confirm this hypothesis, the products of **BDP-2Z** after catalyzed hydrolysis by Cu^{2+} were investigated by UV-Vis and fluorescence spectra. **BDP-2Z** was co-incubated with 10 equiv. of Cu^{2+} in DMF/H_2O followed by UV-Vis and fluorescence detection without any operations. Both the UV-Vis and fluorescence determination results showed that the spectra after adding Cu^{2+} were found to be almost identical to that of **BDP-2**. At the same time, the mixed solution was also determined by ESI-MS analysis and the spectrum showed a main peak at *m*/*z* 699.3237, corresponding to [**BDP-2**+Na]$^+$ (Figure 7). In the meanwhile, there was no peak of [**BDP-2Z** + Na]$^+$ at *m*/*z* 879.3513, which fact implied that **BDP-2Z** had efficiently hydrolyzed into **BDP-2**. Furthermore, an independent amplification reaction was carried out to simulate the recognition process. Treating the reaction mixture with the column chromatography separation method, the main product was obtained and analyzed by ^{1}H NMR spectra which was consistent with that of the **BDP-2**.

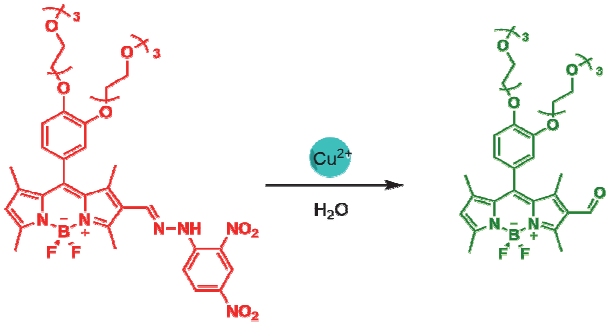

Scheme 2 Recognition mechanism of probe **BDP-2Z** toward Cu^{2+}

To further clarify its recognition mechanism, TD-DFT calculation was performed by Gaussian 09 at PBE0/6-311G (d, p) lever and under DMF as a solvent condition. Multiwfn was used to conduct electron excitation analysis, and the hole-electron analysis and the IFCT (interfragment charge transfer) method were employed simultaneously[31-32]. The electronic absorption maxima of **BDP-2Z** was centered at 548 nm, while the simulated spectra of **BDP-2Z** obtained from time-dependent DFT (TD-DFT) calculation was at 485 nm, ascribed to the $S_0 \rightarrow S_1$ (π-π*) transition of the BODIPY moiety, along with high molar absorption coefficients. Although there was a 63 nm shift between theoretical calculation and the experiment, the result could still explain the experimental absorption spectrum. To examine the possibility of the PET mechanism, at the level of M06-2X/6-311G(d, p), the structure optimization and frequency analysis of the fluorophore and the acceptor were carried out in the DMF solvent environment, respectively. An energy level located between the fluorophores highest occupied molecular orbital (HOMO) and lowest unoccupied molecular orbital (LUMO). Therefore, neither the d-PET mechanism nor the a-PET mechanism supports occurrence.

Subsequently, the possibilities of the ICT process were examined. The electron distribution of the **BDP-2Z** molecule was investigated and the results were as follows. It could be seen in Figure S6a that the holes were mainly distributed on BODIPY and dinitrophenylhydrazine, especially on the two N atoms of the hydrazone. Electrons were also mainly distributed on BODIPY, dinitrophenylhydrazine and its two nitro groups. Combined with the smoothed description of the hole-electron distribution in Figure S6b, the $S_0 \rightarrow S_1$ transition could be assigned as a π-π* characteristic of local excitation and electron transfer. The real-time analysis of the orbital contribution of holes and electrons shows that the hole contribution rate of MO154 (HOMO) was 96.4%, while the electron contribution rate of MO155 (LUMO) was 95.5%.

Then, in order to examine the contribution of each part of the compound to the electronic excitation, the OMe substituent was used to replace the larger polyethyleneglycol (PEG) group, the compound was divided into fragments, and the fragment charge transfer analysis IFCT was performed. The results showed that the contribution of fragment 2 to holes was 60.46%, the contribution of fragment 3 to holes was 39.31%, the contribution of fragment 2 to electrons was 63.58%, and the contribution of fragment 3 to electrons was 34.69%, that is, electronic transitions were mainly carried out in fragment 2 and fragment 3, and the contribution of fragment 1 was very small and could be ignored. There was a bidirectional transfer of electrons between fragment 2 and fragment 3, resulting in a net transfer of 0.04025 electrons from fragment 2 to fragment 3 and 0.00897 electrons from fragment 2 to fragment 1. Comprehensive electron transfer CT accounted for 47.917%, and local excitation LE accounted for 52.083%. The results were consistent with the hole-electron analysis, that the electronic excitation of the compound was mainly composed of local excitation and electron transfer, that is, the $S_0 \rightarrow S_1$ transition refered to the local excitation and electron transfer characteristic of π-π*.

In conclusion, the fluorescence quenching of the probe **BDP-2Z** was caused by ICT (intramolecular charge transfer). After the hydrolysis of the probe by Cu^{2+}, the ICT process was destroyed, resulting in the fluorescence enhancement of the system and the realization of highly sensitive detection.

2.6 Photostability

The photostability of probe **BDP-2Z** and fluorophore BDP-2 was investigated by continuous irradiation with a xenon lamp (150 W) at the corresponding absorption maximum wavelength. The fluorescence intensity of **BDP-2Z** and BDP-2 remained almost unchanged after 30 min of irradiation (retaining more than 98% of the initial fluorescence intensity). The results showed that the probe had sufficient photostability and potential biological application prospects.

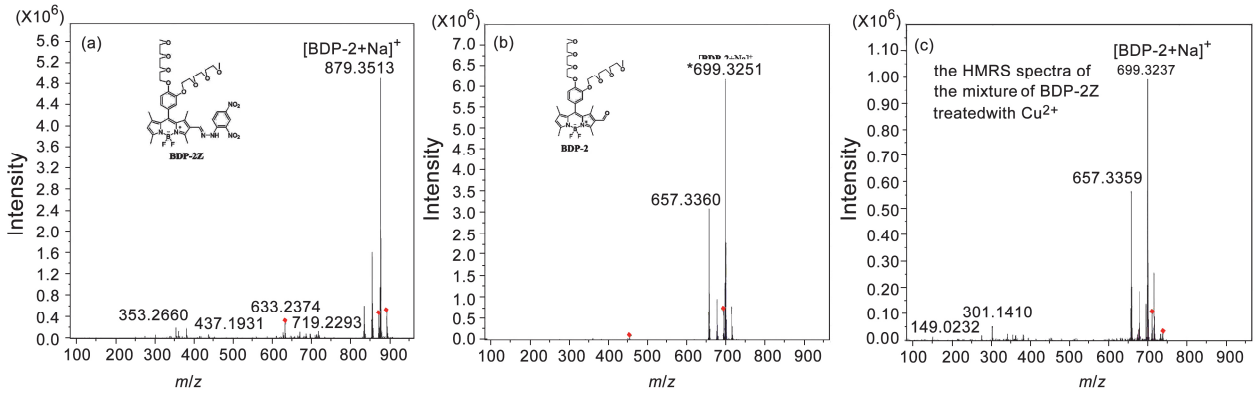

Figure 7 Mass spectrum of probe **BDP-2Z** (a), BDP-2 (b) and the mixture of **BDP-2Z** with addition of Cu^{2+} (c)

2.7 Analytical application in yellow river and tap water samples

Based on the above discussion of the properties of the probe, the sensing ability of the probe to Cu^{2+} in actual water samples was investigated, and the data are shown in Table 1 (The Yellow River water is collected from the upper reaches of Lanzhou Yintan Wetland Park). By monitoring the fluorescence intensity of the probe **BDP-2Z** in river water and tap water with different Cu^{2+} contents, a standard addition recovery test was carried out. All water samples were centrifuged before use. A certain amount of Cu^{2+} (0.5, 2.5 and 5 μmol/L) was added to the water samples. As shown in Table 1, the added concentration of Cu^{2+} ions were very close to the detected concentration, showing good accuracy and precision (RSD＜3%), and the good recovery rate proves that the probe is effective for the detection of Cu^{2+} in water samples. The detection exhibited the practicality of efficient and rapid detection.

Table 1 Determination of Cu^{2+} concentrations in water samples[a]

Sample	Cu^{2+} spiked/ (μmol•L^{-1})	Found/ (μmol•L^{-1})	Recovery/%	RSD/%
River water	0.5	0.52±0.063	105.27	2.60
	2.5	2.53±0.021	100.06	
	5.0	5.14±0.010	102.96	
Tap water	0.5	0.49±0.022	98.44	2.78
	2.5	2.46±0.077	98.71	
	5.0	5.16±0.063	103.33	

[a] Determination of Cu^{2+} ion concentration by compound **BDP-2Z** in real water samples (n=5).

3 Conclusions

A new fluorescent and colorimetric probe **BDP-2Z** was successfully developed for the detection of Cu^{2+} with good water-solubility. The probe not only showed a fluorescence-on recognition process for Cu^{2+}, but also provided a convenient colorimetric detection process without using complicated instruments. The turn-on recognition mechanism was based on the ICT effect before and after hydrolysis reaction of phenylhydrazone. The detection of Cu^{2+} presented well sensitivity and high selectivity under mild conditions, meanwhile, the real-time naked eye detection limit was as low as 5 μmol/L. These properties would widen the application of phenylhydrazone-structured BODIPY derivatives for environment samples.

4 Experimental section

4.1 Materials and measurements

All reagents and solvents were purchased from commercial sources and used without further purification. A stock solution of probe (1 mmol/L) got ready in DMF and the stock solutions of various analytes were provided from LiCl, KCl, $BaCl_2$, $CaCl_2$, CuCl, NaCl, $AlCl_3$, $CrCl_3$, $MnCl_2$, $MgCl_2$, $FeCl_3$•$6H_2O$, $Co(NO_3)_2$•$6H_2O$, $NiCl_2$•$4H_2O$, $AgNO_3$, $ZnCl_2$·$2H_2O$, $CdCl_2$·H_2O, $HgCl_2$, $FeCl_2$, $CuCl_2$•$2H_2O$ (0.1 mmol/L) using deionized water.

The ^1H NMR spectrum and ^{13}C NMR spectrum of the synthesized compounds were measured in $CHCl_3$-d_6 on a Bruck 400 PLUS and DD2 600 MHz spectrometer. The data of absorption spectra and fluorescence spectra were obtained with Beijing Purkinje General T6 UV-vis spectrometer and F97pro fluorescence spectrometer at 25 ℃, respectively. The mass spectra were performed on a Daltonics APEXII 47e FT-ICR of MS spectrometer.

4.2 Experimental method

4.2.1 Synthesis of **2TEG-CHO**

Compound **2TEG-CHO** was synthesized according to previously published literature[41-42]. Add Ts-TEG (8.00 g, 25.00 mmol) to a stirred suspension of 3,4-dihydroxybenzaldehyde (1.38 g, 10.00 mmol), K_2CO_3 (6.91 g, 50.00 mmol) and KI (0.30 g) in dry acetone (200 mL). Stir the resulting mixture at reflux under nitrogen. After the reaction is over, extract with dichloromethane. Dry over sodium sulfate and evaporate to dryness. Chromatograph the residue on silica gel with ethyl acetate (EtOAc) as an eluent then obtain yellow liquid (1.68 g, 90% yield).

4.2.2 Synthesis of BDP

2,4-dimethylpyrrole (2.00 g, 12.00 mmol) and 2TEG-CHO (0.81 g, 6.00 mmol) were dissolved in anhydrous CH_2Cl_2 under argon atmosphere, and added catalytic amount of p-TsOH, the solution was stirred at room tem-

perature until thin-layer chromatography (TLC) analysis showed complete consumption of aldehyde. At this time, DDQ (1.36 g, 6.00 mmol) was added and stirring was continued for 15 minutes, then Et_3N (10 mL) and BF_3•OEt_2 (10 mL) were added. After stirring for an additional 4 h, the crude product was washed three times with water, dried over Na_2SO_4 and concentrated. The residue was chromatographed to give brown oil (1.07 g, 36% yield). ^{1}H NMR (400 MHz, Chloroform-*d*) *δ*: 7.02～6.95 (m, 1H), 6.85～6.75 (m, 2H), 5.96 (s, 2H), 4.24～4.07 (m, 4H), 3.93～3.47 (m, 22H), 3.41～3.30 (m, 6H), 2.53 (s, 6H), 1.45 (s, 6H); ^{13}C NMR (151 MHz, Chloroform-*d*) *δ*: 155.3, 149.6, 149.4, 143.1, 141.5, 131.6, 127.6, 121.1, 121.0, 114.4, 114.2, 71.9, 71.9, 70.9, 70.7, 70.6, 70.5, 70.5, 69.7, 69.7, 69.1, 68.7, 59.0, 59.0, 14.5, 14.5. HRMS (ESI) calcd for $C_{33}H_{47}BF_2N_2O_8$ $[M+Na]^+$ 671.3292, found 671.3299.

4.2.3 Synthesis of BDP-2

Under argon protection and ice-water bath conditions, 3 mL of DMF was added to a 100 mL round-bottomed flask, and then 3 mL of $POCl_3$ was added dropwise. The drop was completed within 15 min, and the reaction was carried out at room temperature for 0.5 h. Subsequently, compound BDP (0.20 g, 0.31 mmol) was added.) was dissolved in 100 mL of DCE, added dropwise to the reaction system, heated to 60 ℃, reacted for 3 h, cooled to room temperature, poured into ice water, slowly added dropwise with 100 mL of saturated $NaHCO_3$ solution, stirred at room temperature for 30 min, extracted three times with dichloromethane, combined the organic phases, dried with anhydrous Na_2SO_4, concentrated, then the residue was separated by column chromatography (PE∶EA = 1∶3, *V*∶*V*) to yield red crystals of BDP-2 (0.19 g, yield 80%). ^{1}H NMR (600 MHz, Chloroform-*d*) *δ*: 10.01 (s, 1H), 7.03 (d, *J*=8.2 Hz, 1H), 6.84 (d, *J*=2.1 Hz, 1H), 6.81 (dd, *J*=8.1, 2.1 Hz, 1H), 6.15 (s, 1H), 4.23 (t, *J*=4.9 Hz, 2H), 4.14 (t, *J*=4.9 Hz, 2H), 3.93 (t, *J*=4.9 Hz, 2H), 3.86 (dd, *J*=5.7, 4.0 Hz, 2H), 3.78 (dd, *J*=5.8, 3.8 Hz, 2H), 3.74～3.50 (m, 15H), 3.39 (s, 3H), 3.36 (s, 3H), 2.82 (s, 3H), 2.61 (s, 3H), 1.75 (s, 3H), 1.52 (s, 3H); ^{13}C NMR (151 MHz, Chloroform-*d*) *δ*: 185.9, 161.5, 156.4, 149.9, 149.9, 147.3, 143.4, 142.8, 134.3, 130.0, 126.6, 123.9, 120.8, 115.3, 114.5, 113.9, 71.9, 71.9, 70.9, 70.9, 70.7, 70.6, 70.5, 70.5, 69.7, 69.6, 69.2, 68.7, 59.0, 59.0, 15.0, 15.0, 13.0, 11.7. HRMS (ESI) calcd for $C_{34}H_{47}BF_2N_2O_9$ $[M+Na]^+$ 699.3241, found 699.3251.

4.2.4 Synthesis of **BDP-2Z**

Compound BDP-2 (0.05 g, 0.07 mmol) and 2,4-dinitrophenylhydrazine (0.03 g, 0.15 mmol) were added to a 100 mL round-bottomed flask, and 30 mL of mixed solvent (EtOH∶EA = 1∶1, *V*∶*V*) was dissolved, 3 drops of acetic acid were added dropwise, then slowly heated to 50°C, the reaction was carried out for 5 h, the mixed solvent was concentrated, then the residue was separated by column chromatography (PE∶EA = 1∶3, *V*∶*V*) to yield purple crystals of **BDP-2Z** (0.07 g, yield 85%). ^{1}H NMR (600 MHz, Chloroform-*d*) *δ*: 11.21 (d, *J*=6.2 Hz, 1H), 9.11 (dd, *J*=5.1, 2.7 Hz, 1H), 8.30 (dt, *J*=9.5, 2.8 Hz, 1H), 8.10 (s, 1H), 7.80 (dd, *J*=9.6, 2.7 Hz, 1H), 7.09～7.02 (m, 1H), 6.88～6.80 (m, 2H), 6.10 (d, *J*=4.7 Hz, 1H), 4.25 (t, *J*=5.0 Hz, 2H), 4.16 (t, *J*=4.9 Hz, 2H), 3.97～3.86 (m, 4H), 3.81～3.51 (m, 16H), 3.39 (d, *J*=1.2 Hz, 3H), 3.35 (d, *J*=1.4 Hz, 3H), 2.81 (d, *J*=6.5 Hz, 3H), 2.59 (s, 3H), 1.69 (d, *J*=3.3 Hz, 3H), 1.50 (d, *J*=5.3 Hz, 3H); ^{13}C NMR (151 MHz, Chloroform-*d*) *δ*: 159.7, 153.9, 149.9, 149.8, 146.1, 144.4, 142.7, 142.3, 139.5, 137.6, 133.4, 130.7, 130.0, 128.8, 126.9, 123.6, 123.1, 122.1, 121.0, 116.5, 114.4, 114.1, 71.9, 71.9, 70.9, 70.9, 70.7, 70.6, 70.6, 70.5, 69.7, 69.7, 69.2, 68.7, 59.0, 59.0, 14.9, 14.1, 12.7. HRMS (ESI) calcd for $C_{40}H_{51}BF_2N_6O_{12}$ $[M+Na]^+$ 879.3524, found 879.3513.

Supporting Information UV-vis and fluorescence spectra of probe **BDP-2Z** and BDP-2; Light stability experiment; **BDP-2Z** and Cu^{2+} in DMF/H_2O solution; DFT calculation data; ^{1}H NMR, ^{13}C NMR and MS spectra of **BDP-2Z**. The Supporting Information is available free of charge via the Internet at http://sioc-journal.cn/.

References

[1] Kirsipuu, T.; Zadoroznaja, A.; Smirnova, J.; Friedemann, M.; Plitz, T.; Tougu, V.; Palumaa, P. *Sci. Rep.* **2020**, *10*, 5686.
[2] Rakshit, A; Khatua, K.; Shanbhag, V.; Comba, P.; Datta, A. *Chem. Sci.* **2018**, *9*, 7916.
[3] Zhang, J.; Duan, D.; Xu, J.; Fang, J. *ACS Appl. Mater. Interfaces* **2018**, *10*, 33010.
[4] Erfanian, A.; Mirhosseini, H.; Rasti, B.; Hair-Bejo, M.; Mustafa, S. B.; Manap, M. Y. A. *J. Agric. Food Chem.* **2015**, *63*, 5795.
[5] Horvath, I.; Blockhuys, S.; Ulskis, D.; Holgersson, S.; Kumar, R.; Burmann, B. M.; Wittung Stafshede, P. *ACS Chem. Neurosci.* **2019**, *10*, 4659.
[6] Zhao, J.; Shi, Q.; Tian, H.; Li, Y.; Liu, Y.; Xu, Z.; Robert, A.; Liu, Q.; Meunier, B. *ACS Chem. Neurosci.* **2021**, *12*, 140.
[7] Wang, X.; Chen, X.; Zhou, R.; Hu, P.; Huang, K.; Chen, P. *Anal. Chem.* **2021**, *93*, 3889.
[8] Kumar, R.; Sharma, A.; Singh, H.; Suating, P.; Kim, H. S.; Sunwoo, K.; Shim, I.; Gibb, B. C.; Kim,J. S. *Chem. Rev.* **2019**, *119*, 9657.
[9] W. Li,; Gong, X.; Fan, X.; Yin, S.; Su, D.; Zhang, X.; Yuan, L. *Chin. Chem. Lett.* **2019**, *30*, 1775.
[10] Chandra, R.; Ghorai, A.; Patra, G. K. *Sens. Actuators*, *B* **2018**, *255*, 701.
[11] Li, X.; Wu, X.; Zhang, F.; Zhao, B.; Li, Y. *Talanta* **2019**, *195*, 372.
[12] Nan, X.; Huyan, Y.; Li, H.; Sun, S.; Xu, Y. *Coordin. Chem. Rev.* **2021**, *426*, 213580.
[13] Wang, Z.; Jia, J.; Zhang, Y.; Chao, J. *Bioorg. Chem.* **2022**, *120*, 105618.
[14] Liu, L.; Dan, F.; Liu, W.; Lu, X.; Han, Y.; Xiao, S.; Lan, H. *Sens. Actuators*, *B* **2017**, *247*, 445.
[15] Zhang, X.; Guo, X.; Yuan, H.; Jia, X.; Dai, B. *Dyes Pigm.* **2018**, *155*, 100.
[16] Aydin, Z.; Yan, B.; Wei, Y.; Guo, M. *Chem. Commun.* **2020**, *56*, 6043.
[17] Wang, X.; Tao, J.; Chen, X.; Yang, H. *Sens. Actuators*, *B* **2017**, *244*, 709.
[18] Gharami, S.; Sarkar, D.; Acharyya, S.; Mondal, T. K. *J. Fluoresc.* **2016**, *26*, 2133.
[19] Wang, S.; Pang, Y.; Xue, M.; Yang, Y. *New J. Chem.* **2021**, *45*, 19219.
[20] Jiao, Y.; Zhou, L.; He, H.; Yin, J.; Gao, Q.; Wei, J.; Duan, C.; Peng, X. *Talanta* **2018**, *184*, 143.

[21] Yang, L.; Tang, A.; Wang, P. *Org. Lett.* **2020**, *22*, 8234.
[22] Liu, C.; Jiao, X.; He, S.; Zhao, L.; Zeng, X. *Org. Biomol. Chem.* **2017**, *15*, 3947.
[23] Liu, K.; Marin, L.; Xiao, L.; Cheng, X. *New J. Chem.* **2021**, *45*, 22888.
[24] Zhao, X.; Gao, C.; Li, N.; Liu, F.; Huo, S.; Li, J.; Guan, X.; Yan, N. *Tetrahedron Lett*. **2019**, *60*, 1452.
[25] Bassan, E.; Gualandi, A.; Cozzi, P. G.; Ceroni, P. *Chem. Sci.* **2021**, *12*, 6607.
[26] Sekhar, A. R.; Sariki, S. K.; Reddy, R. V. R.; Bisai, A.; Sahu, P. K.; Tomar, R. S.; Sankar, J. *Chem. Commun.* **2017**, *53*, 1096.
[27] Zhang, H.; Liu, J.; Sun, Y.; Liu, M.; Guo, W. *J. Am. Chem. Soc.* **2020**, *142*, 17069.
[28] Zhang, Y.; Zheng, X.; Zhang, L.; Yang, Z.; Chen, L.; Wang, L.; Liu, S.; Xie, Z. *Org. Biomol. Chem.* **2020**, *18*, 707.
[29] Chen, H.; He, X.; Su, M.; Zhai, W.; Zhang, H.; Li, C. *J. Am. Chem. Soc.* **2017**, *139*, 10157.
[30] Dunnebacke, T.; Kartha, K. K.; Wahl, J. M.; Albuquerque, R. Q.; Fernandez, G. *Chem. Sci.* **2020**, *11*, 10405.
[31] Lu, T.; Chen, F. *J. Comput. Chem.* **2012**, *33*, 580.
[32] Liu, Z.; Lu, T. Chen, Q. *Carbon* **2020**, *165*, 461.

(Lu, Y.)

